Exploration of the 150 Cavity and the Role of Serendipity in the Discovery of Inhibitors of Influenza Virus A Neuraminidase†

Sankar Mohan and B. Mario Pinto *

Department of Chemistry

Simon Fraser University

8888 University Drive, Burnaby, BC Canada V5A 1S6

†This article is dedicated, with respect and gratitude, to the late Keith Slessor, an inspiring mentor

*****To whom correspondence should be addressed*

bpinto@sfu.ca

Keywords: Influenza A, Neuraminidase enzymes, Inhibitors, Structural analysis

Abstract: Influenza pandemics are an on-going threat for the human population as the avian influenza viruses H5N1 and H7N9 continue to circulate in the bird population and the chance of avian to human transmission increases. Neuraminidase, a glycoprotein located on the surface of the influenza virus, plays a crucial role in the viral replication process and hence, has proven to be a useful target enzyme for the treatment of influenza infections. The discovery that certain subtypes of influenza neuraminidase have an additional cavity, the 150 cavity, near the substrate binding site has triggered considerable interest in the design of influenza inhibitors that exploit this feature. Currently available antiviral drugs, neuraminidase inhibitors oseltamivir and zanamivir were designed using crystal structures predating this discovery by some years. This mini review is aimed at summarizing our group's efforts, together with related work from other groups, on neuraminidase inhibitors that are designed to exploit both the catalytic site and the 150 cavity. The design of a parent scaffold that yields a potent inhibitor which is active in cell culture assays and retains activity against several neuraminidases from mutant strains is also described. Finally, the role of serendipity in the discovery of a new class of potent neuraminidase inhibitors with a novel spirolactam scaffold is also highlighted.

1. Introduction

Influenza infection, caused by influenza viruses A and B, is a respiratory illness characterized by symptoms such as fever, cough, sore throat, weakness and general discomfort.[1] However, the severity of the illness varies significantly depending on the circulating virus and the age and health status of the host.[1] Different strains of influenza virus A are distinguished and characterized by the distinct antigenic properties of two major surface glycoproteins, hemagglutinin (HA) and neuraminidase (NA).[1] Each plays an important and distinct role in the influenza infection cycle. HA mediates the initial attachment of the virus particles to the host cell by interacting with terminal sialic acid residues of the host cell-surface glycans.[2] NA plays a role at a later stage in the infection cycle, it helps the virus to spread from the infected host cell.[3] The budding virions from the infected host cells tend to aggregate on the host cell surface due to the interaction of HA and sialic acid residues present in the cell surface glycan structures. NA, characterized as a sialidase biochemically, cleaves these sialic acid residues and facilitates the release of the newly formed virions from the infected host cell and is thus responsible for continued viral replication. Antigenic variations occur in these surface glycoproteins through a gradual and progressive point mutations (antigenic drift) or complete gene reassortment between two viruses (antigenic shift), for example, complete exchange of the gene segments encoding HA between human and avian influenza viruses.[4] Both antigenic drift and antigenic shift can lead to pandemic outbreaks, the birth of entirely new viral strains for which the human population has no immunity. These outbreaks often result in severe sickness and can cost millions of lives within a short span of time, as evidenced in the past with Spanish flu (1918), Asian flu (1957)

and Hong Kong flu (1968). The Spanish flu in 1918 killed nearly 40-50 million people and the Asian flu (1957) and Hong Kong flu (1968) each claimed an estimated 1-2 million lives.[5] Considering the present-day scenario with changes in the population density and significant increase in air travel, the magnitude of impact could be significantly higher in case of a pandemic outbreak although public health awareness and preparedness have improved significantly.

To date, 18 subtypes of HA and 10 subtypes of NA have been characterized. Among those, 16 subtypes of HA (H1-H16) and 9 subtypes of NA (N1-N9) have been found circulating in birds and H17, H18 and N10 have been found circulating in bats.[1,6] Until 2003, the human population was only exposed to three HA (H1, H2 and H3) subtypes and two NA subtypes (N1 and N2) in the form of human influenza viruses H1N1, H2N2 and H3N2. Although the H5N1virus primarily infects birds, since its first appearance in 1996 (re-emerged in 2003), many human cases of infection have been reported. Between 2003 and May 2017, a total of 453 people died from H5N1-infection or subsequent other infections, about 53% of the total infected cases worldwide.[7] With the first outbreak in early 2013, the world has recently witnessed a total of 5 intermittent epidemic outbreaks of another avian influenza virus, H7N9 that infected humans with a high mortality rate of 30%.[8] In the case of both H5N1 and H7N9 outbreaks, the disease was reported to be contracted by handling infected poultry (bird-to-human transmission). Although human-to-human transmission has not been reported for these avian viruses, a growing concern is that the possibility of genetic reassortment between avian influenza viruses, H5N1 and H7N9 and any of the previously circulating human influenza viruses H1N1, H2N2 and H3N2 could result in a new, highly-virulent strain with the capability of efficient human-to-human transmission.

Annual vaccination offers protection only against previously circulated strains of influenza viruses and will not be effective against infections that are caused by new strains causing the seasonal epidemic or pandemic outbreaks. Owing to its critical role in the viral replication process, neuraminidase has been studied extensively and is a proven target in the treatment of influenza disease. In fact, neuraminidase inhibitors, oseltamivir (**1**)[9] and zanamivir (**2**),[10] are the two block-buster antiviral drugs that have been stockpiled by health authorities throughout the world as part of their pandemic preparedness (Chart 1). Peramivir (**3**, Chart 1)[11] is another neuraminidase inhibitor that was recently approved for the treatment of influenza disease.[12] However, we note that the efficacy of using neuraminidase inhibitors in the treatment or prevention of influenza infections has been questioned.[13] A major challenge in the field of antiviral therapy is the development of drug-resistant mutations in the target enzyme and influenza neuraminidase is clearly not an exception. For example, isolation of an oseltamivir-resistant H5N1 avian influenza virus from a patient indicated viral resistance to these drugs may be increasing.[14] Hence, there exists a constant need for the search for novel antiviral drugs to overcome the multi drug-resistant mutant influenza strains, with the hope that a multi-drug approach will compromise the virus, as with HIV-1 infection.[15] There has been tremendous amount of research focused on the development of neuraminidase inhibitors. In this mini review, we aim to cover recent progress in our own laboratory, together with related work from other groups, with a special focus on a group of neuraminidase inhibitors designed to exploit a newly discovered additional pocket near the active sites of neuraminidase, known as the 150 cavity. We describe also the design of a parent scaffold that yields a potent inhibitor which is active in cell culture assays and retains activity against several neuraminidases from mutant strains.

Finally, the role of serendipity in the discovery of a potent neuraminidase inhibitor with a novel spirolactam scaffold is described.

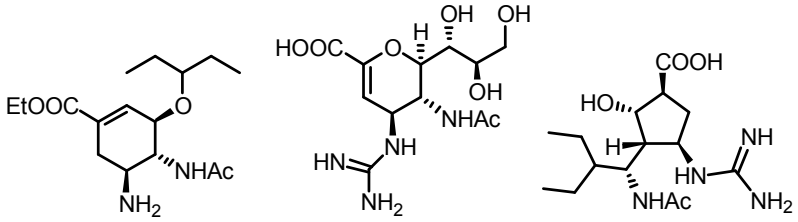

1 oseltamivir **2** zanamivir **3** peramivir

Chart 1. Neuraminidase inhibitors currently in use for the treatment of influenza infection.

2. Neuraminidase crystal structures and the 150 cavity

All known 9 subtypes of neuraminidase are phylogenetically classified into 2 groups. Subtypes N1, N4, N5 and N8 belong to group 1 and N2, N3, N6, N7 and N9 belong to group 2.[16] Determination of three-dimensional crystal structures of N2 and N9 subtypes from group 2, reported in 1983[3c] and 1987,[17] respectively, marked an important milestone in influenza antiviral therapy and greatly facilitated rational drug design. The active site of neuraminidase with highly conserved active-site amino acid residues across all subtypes has been divided into three binding pockets. Pocket 1, composed of residues E276, E277, R292 and N294, interacts with the glycerol side chain of sialic acid. Pocket 2 is composed of hydrophobic residues such as A246, I222, and R224 side chain and interacts with the methyl group of the *N*-acetyl moiety. Pocket 3 is the largest of the three pockets and is formed by many polar residues such as E119, E227, and D151. Structure-based drug design using these crystal structures led to the discovery of oseltamivir (**1**) and zanamivir (**2**). In the absence of crystal structures of group 1 enzymes, a similar catalytic site architecture across all 9 subtypes was assumed, based on the observation that the crystal

structures of N2 and N9 are similar to the crystal structures of phylogenetically more distantly related influenza B neuraminidases.[18] Further supporting this assumption, oseltamivir (**1**) and zanamivir (**2**) were found to be equally active against all subtypes.

However, in 2006, Russell and co-workers[19] crystallized some of the group 1 enzymes (N1, N4 and N8) both in *apo* and *holo* forms and identified substantial active-site conformational differences between group 1 and group 2 enzymes. It was discovered that in the group 1 enzymes, a loop of amino acids (residues 147-152, known as the 150-loop) adopts an unusual conformation. In particular, the side chains of two conserved active-site residues, D151 andE119, adopt different conformations compared to group 2 enzymes. As a result of this unusual conformation of the 150-loop, a new cavity with a dimension of ~10 A° long, 5 A° wide, and 5 A° deep opens up near the catalytic cavity. However, computational studies predicted that the 150 cavity may open to an even greater extent based on a remarkable mobility observed for the 150-loop during simulations.[20] More importantly, the 150 cavity is positioned in such a way that it could be accessible from the catalytic cavity (Figure 1). Hence, it was suggested that group 1 and group 2 subtypes are not only genetically distinct but also structurally distinct. However, subsequent MS simulations and crystallographic studies revealed that even the 150-loop of N2, a group 2 enzyme, also has the flexibility to adopt open conformations.[21] The crystal structure of the N2-oseltamivir complex with a partially open 150-loop suggested that the presence of the 150 cavity is not a unique structural feature of group 1 subtypes but may be applicable to all 9 subtypes.[21b] Exploitation of the 150 cavity for increasing the binding interactions of already existing drugs was suggested as a strategy for the design of potent neuraminidase inhibitors. Since the discovery of the 150 cavity by Russell and co-workers,[19] many neuraminidase

inhibitors have been reported that are designed to take advantage of this additional cavity for increased points of contact in the NA active site.

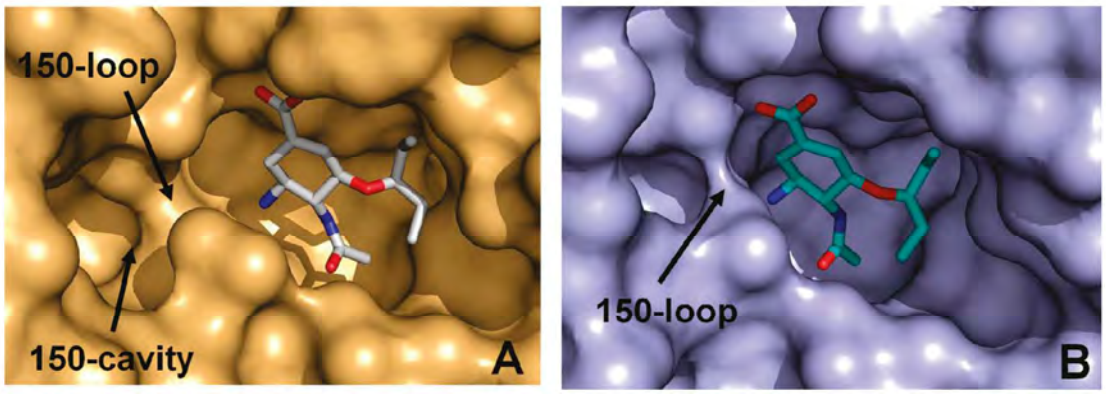

Figure 1. Active site comparison of group 1 and group 2 enzymes: Oseltamivir carboxylate bound in the active site of (A) the N1 subtype and (B) the N9 subtype. Reprinted with permission from Mohan, S.; McAtamney, S.; Haselhorst, T.; Von Itzstein, M.; Pinto, B. M. *J. Med. Chem.* **2010**, *53*, 7377-7391. Copyright © 2010, American Chemical Society.

3. Extension of oseltamivir structure to incorporate 150 cavity binders

The design and syntheses of a series of oseltamivir analogues to target both the 150 cavity and catalytic site were first reported by our group (**3**-**9**, Scheme 1).[22] Since the newly found 150 cavity adjoins the catalytic cavity, we simply extended the structure of oseltamivir by attaching suitable 150 cavity binders using triazole as a linker. Closer inspection of the open loop crystal structure of the N9-oseltamivir complex revealed that the C-5 position with the amino group is suitably positioned towards the 150 cavity and hence was chosen as our modification site. The decision to include a variety of lipophilic groups of different sizes, ranging from simple alkyl chains to a complex steroid moiety, as our potential 150 cavity binders was based on the ensemble-based virtual screening by others.[23] In these computational studies, fragments identified with high affinity scores for the 150 cavity are found to be mainly lipophilic in nature.

Using triazole as a linker allowed us to gain rapid access to different target compounds starting from one key azido intermediate via copper-catalyzed azide-alkyne cycloaddition (CuAAC) of various alkynes carrying potential 150 cavity filling groups. The key azide intermediate **10** was synthesized from D-(–)-quinic acid by following conceptually similar synthetic strategies used in the oseltamivir synthesis.[21] We also synthesized the double bond regioisomer of oseltamivir, iso-oseltamivir **11**,[24] as a parent compound en route to the triazole-extended oseltamivir analogues.[22] Key intermediate **10** was also used to synthesize a novel guanidine compound which turned out to be a potent inhibitor with activity against several mutant strains.[22] Results pertaining to this new candidate are discussed in detail in section 5 (see later).

Inhibitory activities of compounds **3**-**9** against virus-like particles (VLPs) containing a neuraminidase with influenza A/N1 activity ranged from K_i values of 0.07 to 11 μM (Table 1). The K_i values of iso-oseltamivir (**11**, Scheme 1) and zanamivir were determined to be 1.5 and 0.16 nM, respectively, under these assay conditions. To gain more evidence that our compounds indeed access the 150 cavity for binding, the most active compound in the series, compound **4** with a K_i = 70 nM against the N1 containing VLPs (group 1) was screened against N2 (group 2) subtype that was shown to be devoid of this 150 cavity by X-ray crystallography.[22] As expected, compound **4** was found to be 37-fold less active against the N2 subtype, with a K_i value of 2.6 μM. The observed 37-fold selectivity for group 1 enzyme (N1) over group 2 enzyme (N2) together with results from a saturation transfer difference (STD) NMR experiment with compound **4** and N1 containing VLPs allowed us to conclude that the triazole-extended portion of these molecules indeed makes contacts with the 150 cavity of the receptor molecule.[22] Sialic acid-based inhibitors such as zanamivir (**2**) show cross reactivity with some isoforms of the human neuraminidases (hNEU);[25] however, triazole-extended oseltamivir analogues **3**-**9** did not

show significant off-target inhibition against two human neuraminidases, NEU3 and NEU4.[26] However, despite the potent inhibitory activity observed in the functional assay using N1 containing VLPs (K_i = 72 nM for the lead compound **4**), the triazole series did not show significant inhibitory activities at concentrations below 500 μM in the influenza A virus replication inhibition assay performed using two strains (H1N1, Puerto Rico/8/32 and H3N2, Hong Kong/1/68).[27] Although this proof-of-concept series performed as we anticipated and provided a lead compound **4** with nanomolar activity, it still required further optimization to improve its efficacy in cell-based assays.

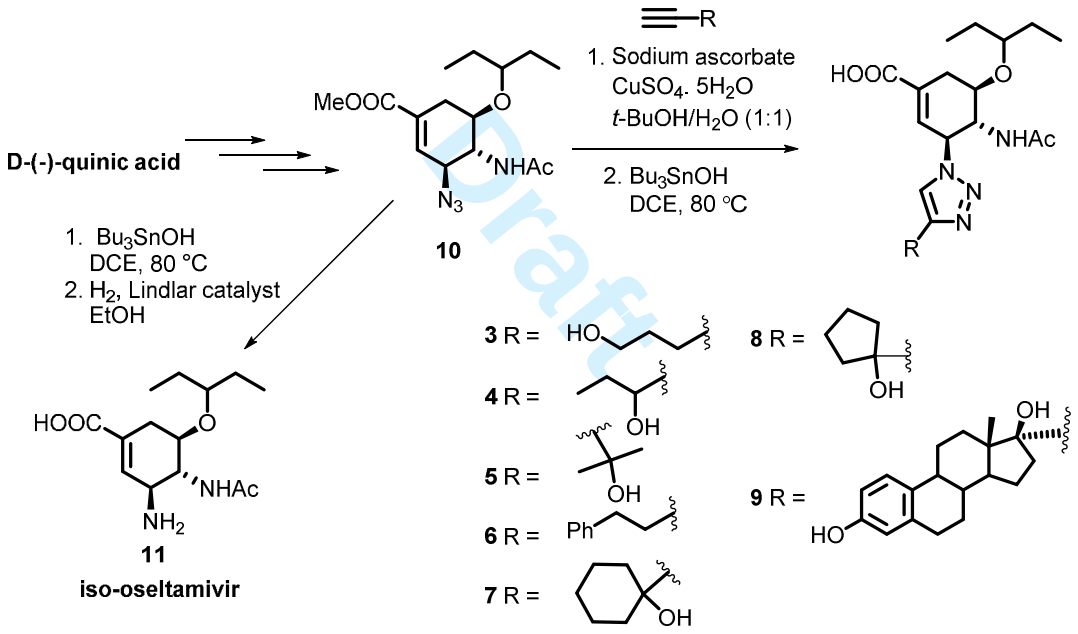

Scheme 1. Synthesis of the first series of neuraminidase inhibitors with 150 cavity binders.[22]

Table 1. Inhibitory activities of compounds **3**-**9**, **11** and zanamivir against N1-containing VLPs[22]

Compound	K_i (*M*)
3	4.6×10^{-7}
4	7.2×10^{-8}
5	1.3×10^{-7}
6[a]	1.2×10^{-6}
7[b]	4.8×10^{-6}
8[b]	1.1×10^{-5}
9[a]	5.8×10^{-6}
11	1.5×10^{-9}
Zanamivir	4.6×10^{-10}

[a] tested as arginine salt, [b] IC_{50} values

To gain further insights into their binding mode, we obtained crystal structures of N8 in complex with three of the triazole-extended inhibitors **3**-**5** and the parent compound **11**.[28] These structures (Figure 2) confirmed that indeed the 150 cavity is occupied and thus provided experimental validation of our design principle. In all three N8-inhibitor complexes, the binding mode of the cyclohexene ring and the interactions in the active site cavity were quite similar to those of the parent compound **11**.[28] However, the triazole portion of the inhibitors adopts two distinct binding modes depending on the substituent at the C-4 position of the triazole ring (Figure 2). In the N8:**3** complex with the 1-hydroxypropyl substituent, the triazole ring is oriented in such a way that the three nitrogen atoms are facing towards the base of the cavity. Surprisingly, this binding mode allowed the 150-loop to close around the triazole group, a feature that was not expected when 150 cavity is occupied. On the other hand, in the N8:**4** and N8:**5** complexes, the triazole ring is rotated by approximately 135° compared to the N8:**3** complex and consequently, the branched alcohol substituents of the triazole ring extend into the 150 cavity. Despite having similar binding modes in the catalytic cavity as that of the parent

compound **11**, reduced inhibitory activities for the triazole-extended oseltamivir analogues in the influenza A virus replication inhibition assay suggested that the new interactions gained within the 150-loop and cavity do not fully compensate for the strong hydrogen bonding network that was compromised by the installation of the less basic triazole ring in place of the parent amino group.[28] This observation was corroborated by the long-term molecular dynamics (MD) simulation study, performed by us, which suggested that the 150 cavity filling group is not stable in the 150 cavity but exits the cavity periodically, thus affecting the overall binding affinity.[29]

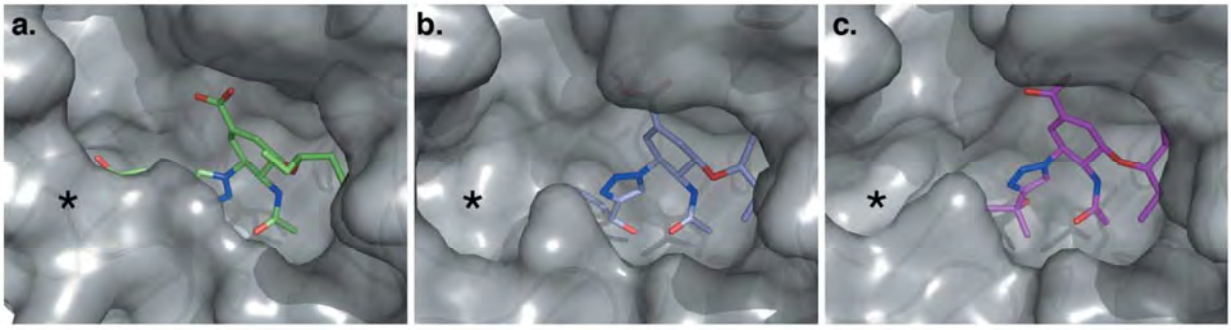

Figure 2. Surface representations of the enzyme active site in N8 inhibitor complexes showing two distinct binding modes for the triazole-extended oseltamivir analogues. (a) **N8:3** complex with 150-loop closed conformation (b) and (c) **N8:4** and **N8:5** complexes with open loop conformation. Reprinted with permission from Kerry, P. S.; Mohan, S.; Russell, R. J. M.; Bance, N.; Niikura, M.; Pinto, B. M. *Sci. Rep.* **2013**, *3*, 2871. Copyright © 2013, Nature Publishing Group.

We therefore designed and synthesized the second-generation inhibitors **12** and **13** in which we shifted the triazole extension to the C-6 position in the oseltamivir scaffold (Scheme 2).[30] The rationale for this design was two-fold: (i) to restore the missing hydrogen bond network

with D151 and E119 residues by keeping an intact amino (**12**) or guanidino group (**13**) at C-5 and (ii) to exploit the 150 cavity with the triazole-extension for new interactions. As opposed to our first-generation inhibitors, the second-generation inhibitors have the double bond in the same place as in oseltamivir, which makes them true oseltamivir analogues. We have utilized the azide intermediate **10** from the first series for the synthesis of second-generation inhibitors **12** and **13**. Target compounds were synthesized using dihydroxylation, azidation of the allyl acetate via allylic azide [3,3]-sigmatropic rearrangement, and copper-catalyzed azide-alkyne cycloaddition as key steps (Scheme 2).[30]

As conjectured, the second-generation triazole-extended oseltamivir analogues (**12** and **13**) showed better inhibitory effects in the virus replication inhibition assay compared to the first-generation inhibitors (**3-9**). When screened against H3N2 (Hong Kong/1/68) strain, compounds **12** and **13** showed inhibitory effects at 100 μM and 20 μM, respectively.[30] However, both compounds did not show inhibitory effects against the H1N1 (Puerto Rico/8/32) strain even at a concentration of 10^{-4} M. MD-simulation studies of compounds **12** and **13** in complex with N1 and N8 crystal structures provided further insights in their binding modes and a possible explanation for their reduced inhibitory compared to standard inhibitors, oseltamivir and zanamivir.[30] There seemed to be a "see-saw effect" operating between the triazole ring and the carbocycle portion. MD simulations indicated ligand movement between two different conformations, one in which interactions of the carbocycle portion (oseltamivir scaffold) in the active site cavity forces the triazole-extended portion to eject into solution and another conformation in which the triazole-extended portion enters the 150 cavity or slides under the D151 but ejects the oseltamivir-like portion from the catalytic site (Figure 3).[30]

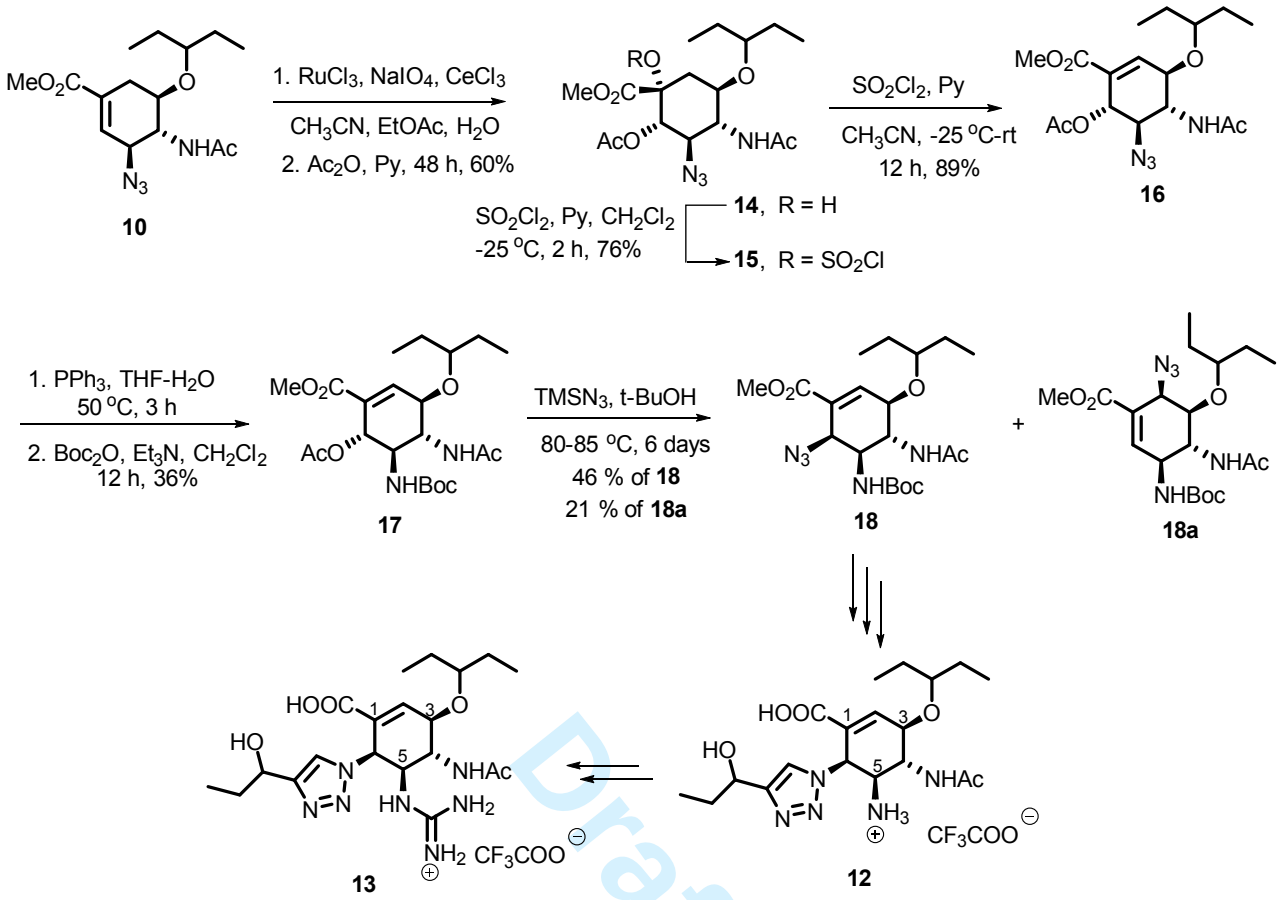

Scheme 2. Synthesis of second-generation triazole-extended oseltamivir analogues.[30]

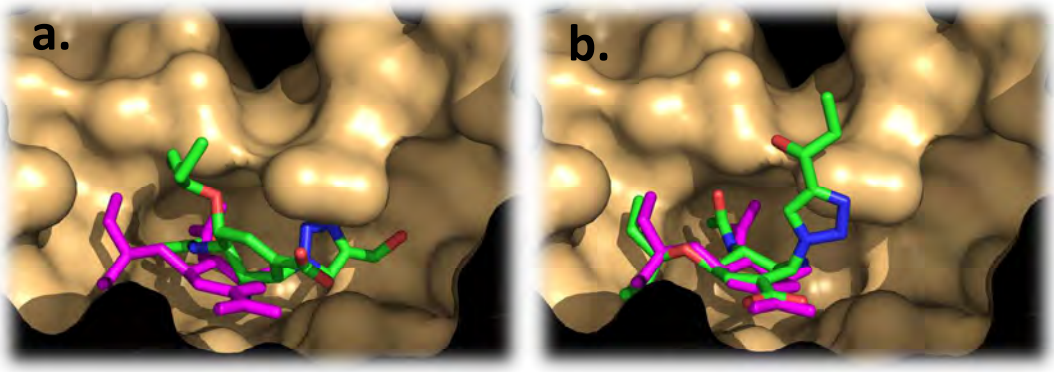

Figure 3. Overlay of MD poses of triazole-extended oseltamivir analogue **13** with N8-oseltamivir complex. (a) conformation showing the triazole portion inside the 150 cavity with the carbocycle ejected from the catalytic cavity (b) conformation showing the carbocycle inside the catalytic cavity with the triazole portion ejected from the150 cavity.

Mooney *et al*.,[31] reported a series of oseltamivir analogues carrying a variety of *N*-substituted guanidino groups as potential 150 cavity binders **19** (Chart 2), but the results were disappointing. The *N*-substituents were a range of alkyl groups containing a maximum of 3 carbon atoms (**19**), methyl (**20**), and hydroxyl (**21**) groups. However, none of derivatives with larger *N*-alkyl groups (**19**) were found to be active in *in vitro* neuraminidase inhibition assays at concentrations below 1 μM, suggesting that modification at the terminal nitrogen atom of the guanidine group is not a viable option to access 150 cavity and still maintain activity. However, this study did identify two potent catalytic site binders, *N*-methyl and *N*-hydroxy guanidine derivatives (**20** and **21**) with low nanomolar activities against both wild-type and H274Y mutants in *in vitro* neuraminidase inhibition assays.[31] It was clearly demonstrated by docking studies that these two inhibitors (**20** and **21**) interact only within the catalytic cavity and don't make any interactions in the 150 cavity, because neither the *N*-hydroxyl group nor the *N*-methyl group were large enough to extend beyond the catalytic cavity.

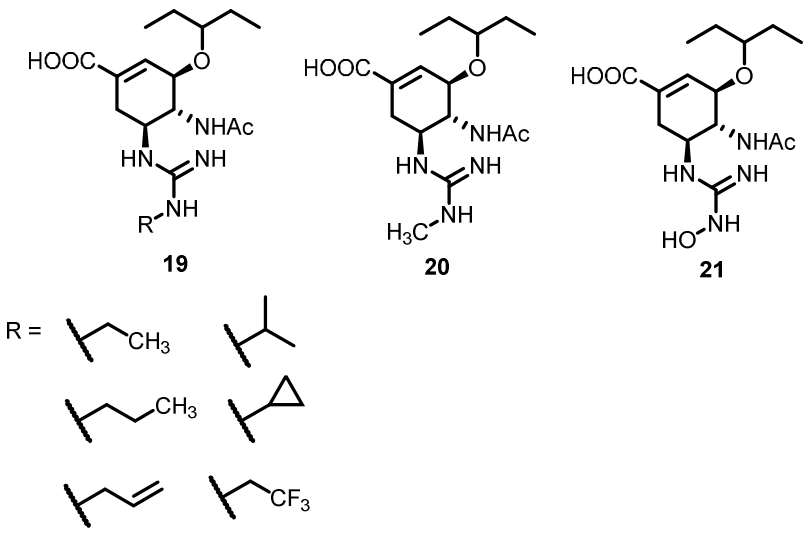

Chart 2. *N*-substituted guanidine analogues of oseltamivir.[31]

In 2014, Xie et al.,[32] reported the design and synthesis of two series of oseltamivir analogues carrying a variety of 150 cavity binders. The first series contained different 150 cavity filling groups at the internal nitrogen atom of a guanidino group at the C-5 position of oseltamivir (**22**, Chart 3) whereas the second series carried different *N*-alkylated secondary amino functions (**23**, Chart 3). The *N*-substituted guanidine series (**22**) showed less inhibitory activity than the parent guanidine analogue of oseltamivir (**24**), indicating that *N*-alkylation of the guanidino group is detrimental to inhibitory activity. However, the second series with *N*-alkylated secondary amino functions at C-5 furnished several potent inhibitors. More importantly, compound **25** with IC_{50} values of 1.9, 3.8, and 6.7 nM against three types of H5N1-NAs (*in vitro* neuraminidase inhibition assays) is the most active compound discovered to date among the oseltamivir-based neuraminidase inhibitors designed to target both the catalytic site and 150 cavity.[32] Compound **26** was the second-best inhibitor in the series, with IC_{50} values of 2.1, 4.3 and 14 nM against three types of H5N1-NAs. Both compounds were highly selective for the N1 (group 1) over N2 (group 2) enzyme, with IC_{50} values in the micromolar range against

two types of H9N2-NAs screened, suggesting that these compounds were utilizing both the catalytic site and 150 cavity for binding. Docking studies also corroborated the binding pose for these compounds, which snuggly fit across both sites. Importantly, compound **25** was ~8-fold and ~3-fold more active than oseltamivir (**1**) and the guanidine analogue of oseltamivir (**24**), respectively. However, as with oseltamivir, compound **25** showed ~1000-fold decrease in inhibitory activity against H5N1-NA carrying the oseltamivir-resistant H274Y mutation (IC_{50} for **25** = 1.16 μM and IC_{50} for oseltamivir = 2.1 μM).[31] On the other hand, compound **26** was found to be less affected by the H274Y mutation compared to compound **25** and oseltamivir. The IC_{50} value of compound **26** against the H274Y-mutant was determined to be 160 nM, that is, less than 80-fold decrease in inhibitory activity compared to the wild-type inhibition. Clearly, these results suggest that exploitation of the 150 cavity is a viable strategy in the search for next-generation neuraminidase inhibitors.

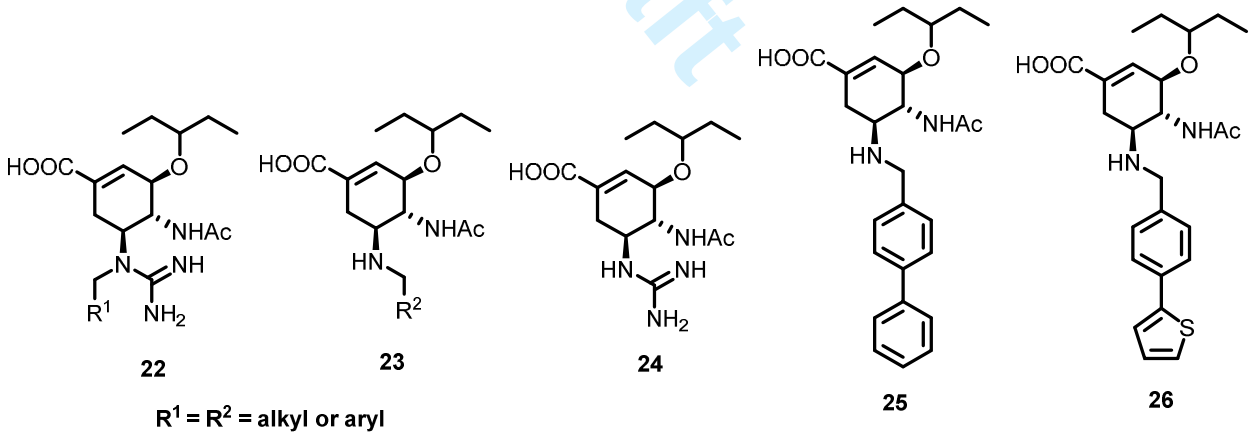

Chart 3. Novel oseltamivir analogues with 150 cavity binders.[32]

4. Extension of zanamivir structure with 150 cavity binders

Using a molecular modeling approach, Wen *et al.*,[33] reported the first series of zanamivir analogues that are intended to target both the catalytic site and 150 cavity (Chart 4). The design included a series of 150 cavity binders attached either to the terminal (**27a,b**) or the internal nitrogen (**28a-c** and **29a-d**) atom of the guanidino function of zanamivir and another series in which C-4 position of 2-deoxy-2,3-didehydro-*N*-acetylneuraminic acid (DANA) was modified with a secondary amino function carrying different 150 cavity groups (**30a-d**). However, none of the *N*-alkylated DANA analogues (**30a-d**) showed significant inhibitory activities. In contrast, in the *N*-alkylated guanidine series (**27**, **28** and **29**), compound **29a** bearing a 3-(piperazinocarbonyl)-propyl substituent was shown to be effective both in the neuraminidase inhibition assay (IC_{50} = 2.15 μM) as well as in the influenza virus replication assay (EC_{50} = 0.77 μM), but the inhibitory activities were still inferior to that of zanamivir (IC_{50} = 4 nM and EC_{50} = 13 nM).[33]

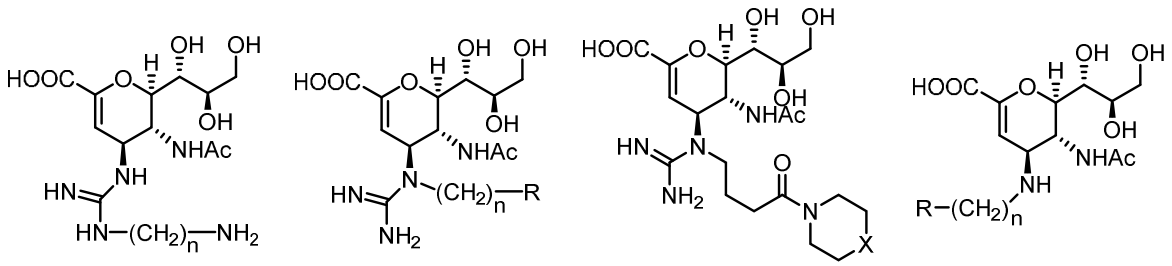

Chart 4. Novel zanamivir analogues with 150 cavity binders.[33]

Rudrawar *et al.*[34] reported a multidisciplinary approach for the design and characterization of novel sialic acid analogues carrying 150 cavity binders at the C-3 position (**31** and **32**, Chart 5) using molecular modelling, chemical synthesis, enzyme and cell-based assays,

and protein X-ray crystallography. The target compounds were synthesized from the per-acetylated derivative (**34**) of DANA via allylation at C-3 followed by deprotection (**31**) or allylation at C-3 followed by olefin cross-metathesis and deprotection (**32**), as shown in Scheme 3.[34] In a fluorometric assay, both target compounds (**31** and **32**) showed selective inhibition of group 1 sialidases (wild-type N1 and mutant N1) over group 2 sialidase (N2) while the parent compound DANA (**33**) lacking the 150 cavity binder showed comparable inhibition of both group 1 and group 2 enzymes. The selective inhibition of N1 over N2 subtype exhibited by the C-3 modified DANA analogues, **31** and **32**, was also confirmed by the plaque reduction assay. Compound **32** was more active than the allyl derivative **31**. Through X-ray crystal structures of **31** and **32** in complex with the N8 subtype, it was clearly demonstrated that the C-3 extension with appropriate groups leads to occupation of the 150 cavity formed by an open loop conformation (Figure 4).[34] In both N8-**31** and N8-**32** complexes, the binding pose of the dihydropyran ring overlays very well with that of DANA in the catalytic site while the C-3-extended groups, allyl or (*p*-tolyl)allyl, were protruding into the 150 cavity, which locks the 150-loop in an open conformation as anticipated (Figure 4).

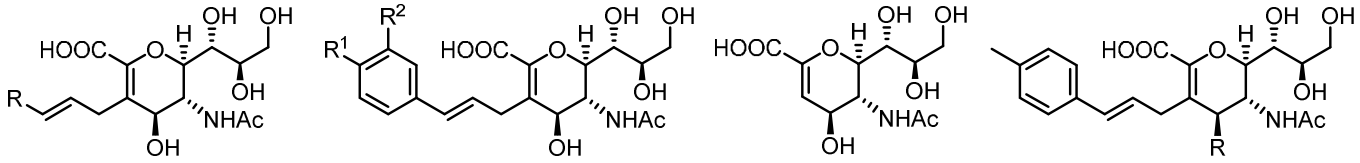

31 R = H
35 R = *t*-Bu
36 R = cyclohexyl
37 R = naphthyl
38 R = 3,4-dimethoxybenzyl

32 $R^1 = CH_3$, R^2 = H
39 $R^1 = R_2$ = H
40 R^1 = COOH, R^2 = H
41 $R^1 = CH_3$, R^2 = COOMe
42 $R^1 = CH_3$, R^2 = COOH
43 R^1 = OtBu, R^2 = H

DANA (**33**)

44 R = NH_2
45 R = NHC(NH)NH_2

Chart 5. Novel C-3-extended analogues of zanamivir developed by Rudrawar *et al*.[34,35,36]

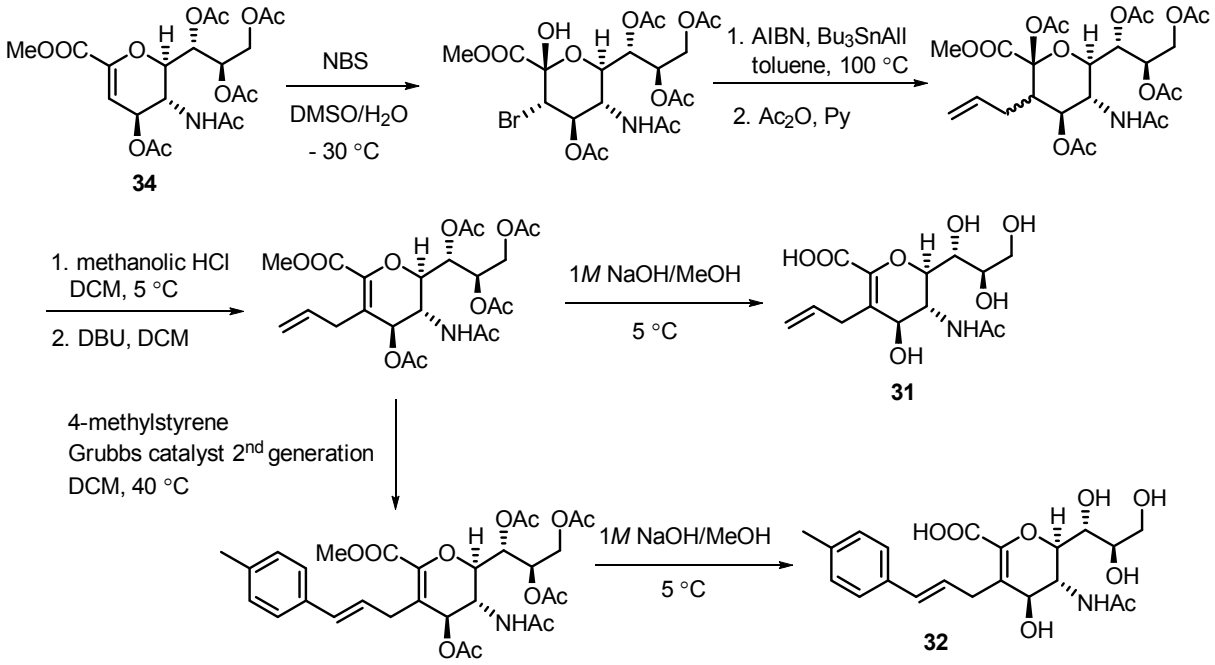

Scheme 3. Synthesis C-3 extended analogues of zanamivir.[34]

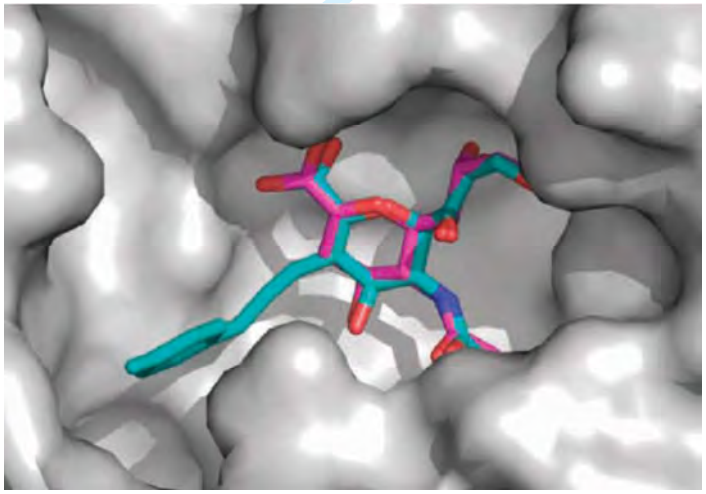

Figure 4. Superimposition of N8: **32** complex with N8: DANA (**33**) complex.[34] Reprinted with permission from Rudrawar, S.; Dyason, J. C.; Rameix-Welti, M.-A.; Rose, F. J.; Kerry, P. S.; Russell, R. J. M.; van der Werf, S.; Thomson, R. J.; Naffakh, N.; von Itzstein, M. *Nat. Commun.* **2010**, *1*, 113. Copyright © 2010, Nature Publishing Group.

Despite the success in accessing both catalytic site and 150 cavity, there was no increase in the inhibitory activity of **32** compared to the parent compound DANA (**33**). Subsequent work to improve this scaffold using substituted aromatic moieties or bulky aliphatic groups at the terminal position of the C-3 allyl extension (**35-43**, Chart 5) was not successful and resulted in compounds with either comparable or weaker inhibitory activities to that of **32**.[35] Rudrawar et al.,[36] also reported an interesting study in which they synthesized amino (**44**) and guanidino (**45**) derivatives of compound **32** (Chart 5) and tested them against an atypical group 1 enzyme (N1 from pdm09-H1N1), and a group 2 enzyme (N2 from pdm57-H2N2), which were shown to lack the 150 cavity by crystallography. Both amino derivative **44** and the parent compound **32** showed comparable inhibitory activities (IC_{50} = 3.5 and 6.5 μM, respectively) against N1 sialidase (pdm09 H1N1). Compound **32** was previously shown to inhibit other group 1 enzymes with a 150 cavity at a similar level.[34] However, guanidine substitution (**45**) resulted in a 100-fold decrease in inhibitory activity (IC_{50} = 336 μM).[36] Surprisingly, both compounds **44** and **45** showed 10-fold greater inhibitory activities (IC_{50} = 0.1 and 42 μM, respectively) against N2 compared to N1 sialidase. This observation was in direct contrast with their designed purpose and provided the first *in vitro* evidence further strengthening previous findings by computational and crystallographic studies,[21] that even the 150-loop of group 2 enzymes and atypical group 1 enzyme, N1 from 2009 pandemic H1N1 virus (09N1) also have the flexibility to adopt open conformations. Subsequently, X-ray crystal structures of compound **32** in complex with 09N1 and the 09N1-I149V mutant showed that inhibitor **32** was indeed occupying both the catalytic site and 150 cavity, forcing a half-open loop conformation that was not previously seen in the 09N1crystal structure.[37]

In 2013, Lin et al. [38] reported the synthesis and biological activities of a library of acylguanidine zanamivir analogues (**46**, Chart 6). From this library of more than 30 compounds, compound **47**, with nanomolar level inhibitory activity against both N1 and N2 (IC_{50} = 20.1 and 25.5 nM, respectively) was identified as a lead compound. The binding pose for compound **47** predicted using computer docking studies was also in agreement with occupation of the 150 cavity by the intended hydrophobic acyl substituent on the guanidine function. Further refinement of this series was achieved by swapping the naphthyl group with a variety of 4-substituted triazole rings (**48**, Chart 6).[39] Most compounds from the triazole series exhibited inhibitory activities below 15 nM against N1 and N2 subtypes. Compound **49** with a cyclohexyl substituent on the triazole ring was found to be the most potent compound in the series, with IC_{50} values of 2.3 and 2.9 nM against N1 and N2, respectively.[39] We also note that compound **49** is the most active compound discovered to date among the zanamivir-based neuraminidase inhibitors that are designed to target both the catalytic site and 150 cavity.

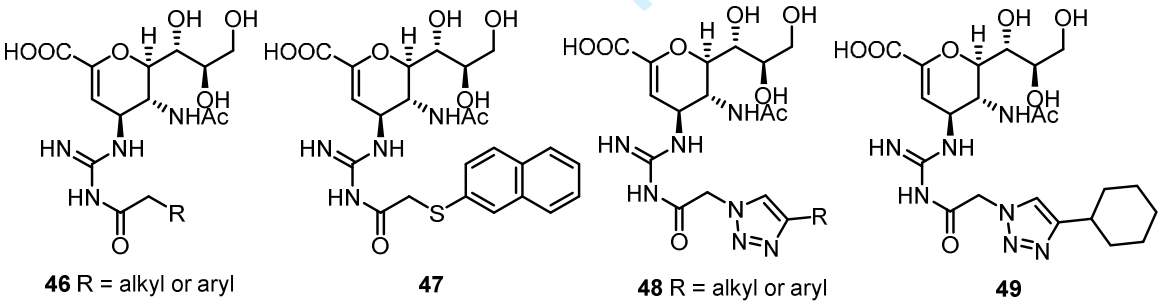

Chart 6. Acylguanidine zanamivir analogues and further optimized triazole series.[38,39]

5. Discovery of carba-zanamivir and a novel spirolactam scaffold

In the discovery process of zanamivir (**1**), guanylation of the 4-amino derivative of DANA (**50**) resulted in 100-fold increase in the inhibitory activity.[10] The K_i value for zanamivir with a guanidine group at C-4 (zanamivir numbering) was 0.1 nM whereas the parent compound, the 4-amino derivative of DANA had a K_i value of 10 nM.[10] However, in the case of oseltamivir (**1**) guanylation of the C-5 amino group **51** (oseltamivir numbering) didn't have a significant effect and showed only a 5-fold increase in activity (IC_{50} value 1 nM vs 0.2 nM).[24] We hypothesized that in the case of zanamivir, the increase in inhibitory activity upon guanylation could be due to the position of the double bond that is different from oseltamivir. Hence, we decided to utilize the key azido intermediate **10**,[22] used in the synthesis of our first generation 150 cavity inhibitors, to derive a carbocyclic analogue of zanamivir (**52**) with structural features of both oseltamivir and zanamivir (Scheme 4 and 5). This hybrid inhibitor resembles the zanamivir core structure with respect to all the substituents on the cyclohexene ring including the position of the double bond, *except* that the D-glycero side chain has been replaced with the lipophilic 3-pentyloxy group of oseltamivir.[22]

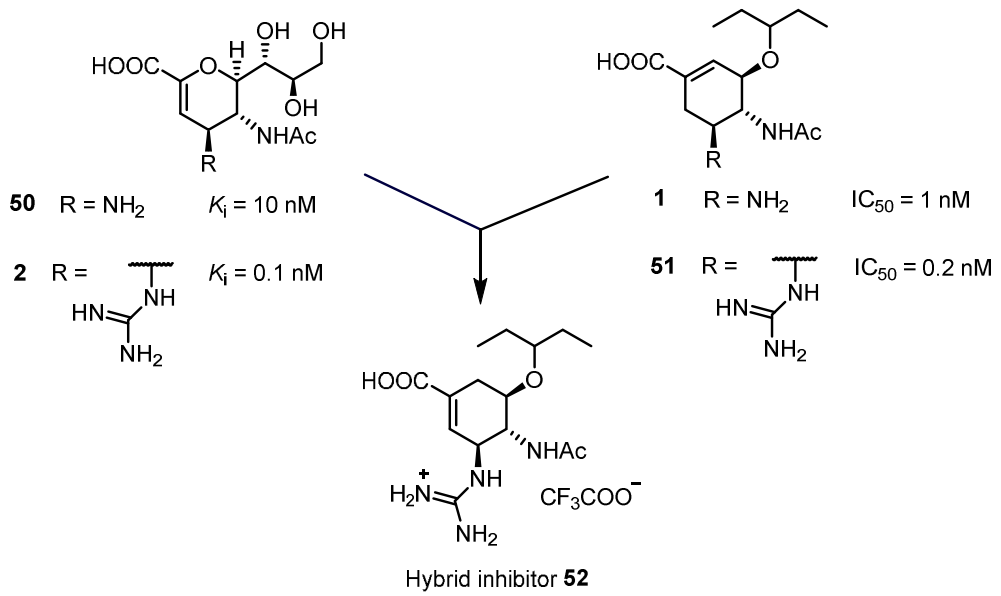

Scheme 4. Genesis of the carbocyclic analogue of zanamivir **52**[22]

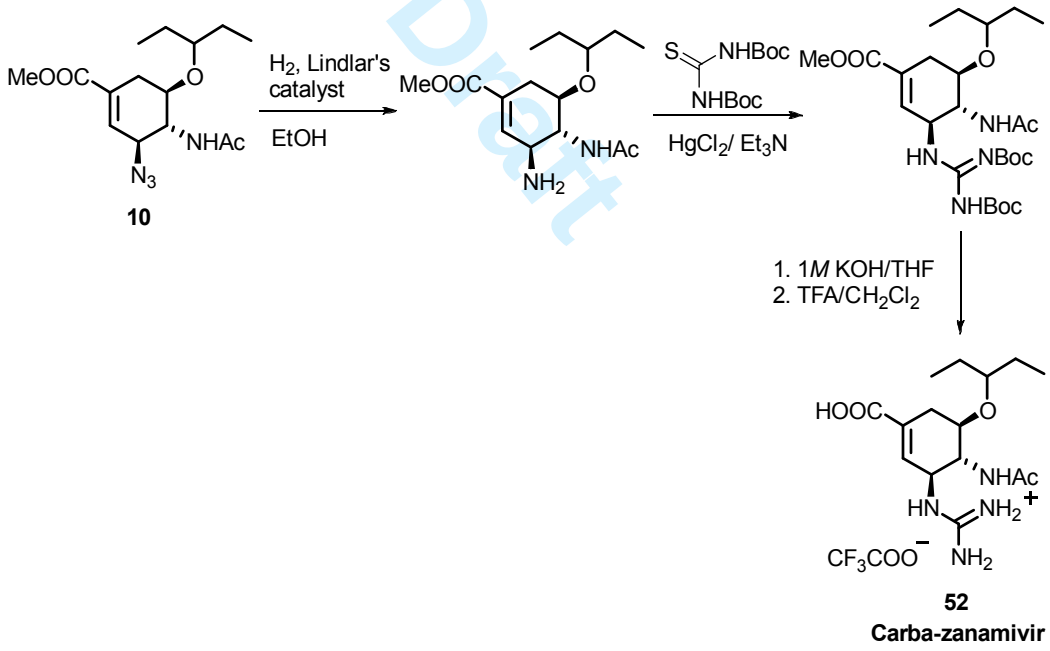

Scheme 5. Synthesis of the carbocyclic analogue of zanamivir **52**.[22]

In the functional assay using VLPs containing N1 activity, compound **52** exhibited comparable inhibitory activity (K_i = 0.46 nM) to that of zanamivir (K_i = 0.16 nM).[22] It also

showed excellent inhibitory activity in the influenza virus replication assay against two strains H3N2 (Hong Kong/1/68) and H1N1 (Puerto Rico/8/32).[27] Similar to standard inhibitors oseltamivir and zanamivir, compound **52** inhibited both strains at less than μM concentrations. It also exhibited very high selectivity for viral neuraminidases over human neuraminidases.[26] When tested for the off-target effect of this compound against human sialidases, isoforms NEU3 and NEU4. compound **52** didn't show measurable inhibition below 1 mM concentrations against these human sialidases. This selectivity is crucial for any anti-viral agent to avoid adverse side effects resulting from potential off-target inhibition of human neuraminidases which recognize similar substrates.

Significantly, the hybrid inhibitor **52** showed reduced susceptibility to the oseltamivir-resistant H274Y mutation.[28] The mechanism of oseltamivir resistance by H274Y mutation was well established by crystallographic studies.[40] The H274Y mutation confers changes in the lipophilic pocket that interacts with the 3-pentlyoxy side chain of oseltamivir and consequently the pentyloxy group shifts 2 Aº out of the enzyme active site which, in turn, makes other groups around the cyclohexene ring shift from their optimal positions. Peramivir (**3**), having a 3-pentyl sidechain is also affected by this mutation (100-fold).[41] When screened against A/Brisbane/59/2007 (oseltamivir-sensitive, wild-type), the hybrid inhibitor **52** exhibited a lower EC_{50} value of 3.9 μM than oseltamivir (EC_{50} = 12 μM).[28] Surprisingly, the H274Y mutation had a lesser effect on the inhibitory activity of compound **52**. Despite having the same 3-pentyloxy group as oseltamivir, it only required a 10-fold higher concentration to inhibit A/Brisbane/59/2007-like oseltamivir resistant (H274Y) strain than required for the inhibition of the wild-type strain (EC_{50} = 34 μM compared to 3.9 μM).[28] Oseltamivir did not show inhibition of virus replication at concentrations up to 500 μM against this mutant strain.[28]

The crystal structure of N8 in complex with the hybrid inhibitor[28] and MD-simulations[29] provided explanations for the observed potent inhibitory activity of this compound and its reduced susceptibility towards H274Y mutation. Examination of the crystal structure of the N8:**52** complex indicated that the overall binding mode and the interactions of the groups around the cyclohexene ring with the active site residues generally overlay very well with the N8: oseltamivir complex (Figure 5).[28] The guanidine group adopts a similar position as seen in the N8: zanamivir complex and makes additional hydrogen bond interactions with carboxyls of E119 and E227 and the backbone carbonyls of W178 and D151. Such a strong hydrogen-bond network surrounding the guanidino group in addition to the usual interaction of the carboxylate moiety with the arginine triad seem to anchor the hybrid inhibitor in the active site. Based on these observations and our MD-simulation studies, we proposed that the hybrid inhibitor can pivot about these two-anchoring points in response to a H274Y mutation without lifting the entire ligand out of the active as opposed to what was seen in the oseltamivir case, thus explaining its reduced susceptibility towards H274Y mutation. We note, however, that the reduced susceptibility of **52** towards H274Y mutation is not just the effect of guanylation alone because the guanidine derivative of oseltamivir **51** was found to be sensitive to the H274Y mutation to the same extent as oseltamivir.[42] Therefore, it is the combined effect of both change in position of the double bond relative to oseltamivir and the guanidine function which allows this new scaffold to overcome the H274Y mutation.

A

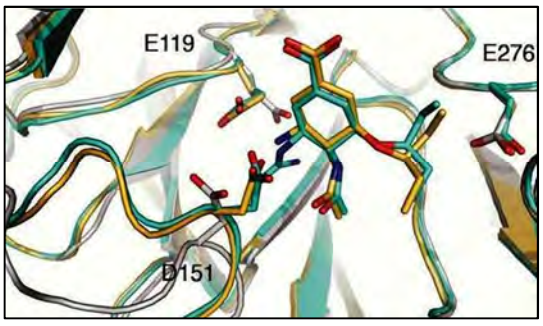

B

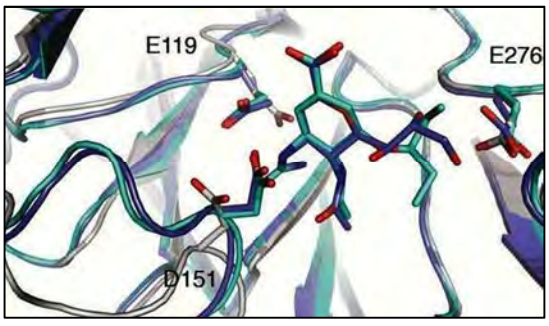

Figure 5. Overlay of the active site of the N8:**52** complex with that of (A) the N8:oseltamivir complex. (B) the N8:zanamivir complex.[28] Reprinted with permission from Kerry, P. S.; Mohan, S.; Russell, R. J. M.; Bance, N.; Niikura, M.; Pinto, B. M. *Sci. Rep.* **2013**, *3*, 2871. Copyright © 2013, Nature Publishing Group.

When screened against drug-resistant mutations in the N2 subtype, compound **52** continued to maintain a better inhibitory profile than oseltamivir.[43] The K_i values of oseltamivir, zanamivir, and the hybrid inhibitor **52** for the inhibition of wild-type N2 were 0.21, 0.14 and 0.18 nM, respectively. There was only a 3.8 and 4.8-fold increase in K_i values for zanamivir and compound **52**, respectively, against the E119V single mutant, whereas oseltamivir had a 50-fold increase in its K_i value. Another single mutation, I222L did not have a significant effect on the inhibitory activities of all three inhibitors. But when present in combination with E119V as a double mutant (E119V/I222L), it brought significant resistance to oseltamivir (252-fold increase in K_i value compared to wild type), but only a 36 and 37-fold increase in K_i values for compound **52** and zanamivir, respectively. Once again, it was evident from the analysis of the crystal structures of wild-type N2 and the corresponding single (E119V and I222L) and double mutants (E119V/I222L) in complex with hybrid inhibitor **52**, oseltamivir and zanamivir that the strong hydrogen-bond network surrounding the guanidine group in the case of compound **52** and zanamivir allows them to escape these drug resistant mutations.[43] For example, I222L mutation weakens the hydrophobic interactions with the 3-pentyloxy side chain of oseltamivir which is also the case for compound **52** (MS-257); however, this mutation alone doesn't have a significant effect on inhibitor potency. But, when present together with E119V (a E119V/I222L double mutation), oseltamivir's inhibitory activity decreases 252-fold against this double mutant

due to the loss of a salt bridge with D151 and the amino group. In the case of compound **52**, the salt bridge is retained between guanidine and E227 and D151 residues, thus explaining the better inhibitory activity of this compound compared to oseltamivir against these mutations (Figure 6).[43] Furthermore, compound **52** also showed potent inhibition of neuraminidases from H7N9 and H1N1 strains with comparable IC_{50} values to that of oseltamivir and zanamivir (Table 2).[44,45] Thus, the hybrid inhibitor **52** has an excellent inhibitory profile against a panel of influenza neuraminidases and remains resilient towards drug-resistant mutations both in N1 and N2 subtypes (Table 2) which makes it an ideal candidate for further optimization.

Table 2. Summary of in vitro inhibitory activity of the hybrid inhibitor **52** against various wild type and mutant neuraminidases compared to oseltamivir and zanamivir (nM).[22, 43-46]

	(H5)N1-VLPs[a]	**(H2)N2-WT**[a]	**(H2)N2-E119V**[a]	**(H2)N2-I222L**[a]	**(H2)N2-E119V/I222L**[a]	**(H7)N9**[b]	**H1N1**[b]	**H1N1-H274Y**[b]
52	0.46	0.18	0.87	0.50	6.48	1.09	0.74	707.8
Oseltamivir	n.d.	0.21	10.61	0.90	48.72	0.79	1.04	2376
Zanamivir	0.16	0.14	0.49	0.30	5.26	0.41	0.95	1.31
Reference	*22*	*43*	*43*	*43*	*43*	*44, 46*	*45*	*45*

[a] K_i values; [b] IC_{50} values; n.d. = not determined.

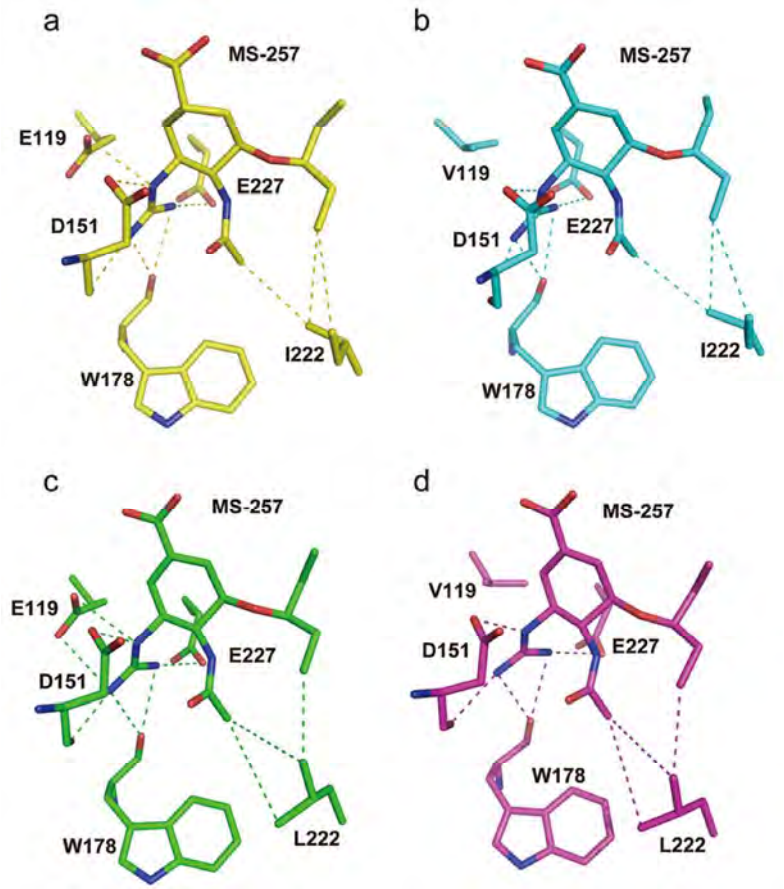

Figure 6. Binding modes of **52** in complex with N2, depicting active site interactions affected by different mutations (a) Wild-type N2: **52** complex (b) E119V mutant:**52** complex (c) I222L mutant:**52** complex (d) E119V/I222L double mutant:**52** complex.[43] Reprinted with permission from Wu, Y.; Gao, F.; Qi, J.; Bi, Y.; Fu, L.; Mohan, S.; Chen, Y.; Li, X.; Pinto, B. M.; Vavricka, C. J.; Tien, P.; Gao, G. F. *J. Virol.* **2016**, *90*, 10693-10700. Copyright © 2016, American Society for Microbiology.

During the course of further optimization of the lead compound **52**, we serendipitously discovered a novel spirolactam scaffold with potent neuraminidase inhibitory activity.[47] Our original intention was to synthesize the isothiourea version (**53**) of the hybrid inhibitor **52**. The synthetic approach to this target compound involved nucleophilic ring opening of the *N*-Acetyl

aziridine intermediate **54** using Boc-protected thiourea, followed by hydrolysis of the methyl ester and deprotection of the Boc-protecting group, as shown in Scheme 6. However, we isolated two diastereomeric spirolactams **55** and **56** instead of the desired target compound **53**. We have explained the formation of this spirolactam ring from the coupled product **58** via base-catalyzed double bond migration followed by lactamization, facilitated by the conditions employed in the ester hydrolysis step (Scheme 7).[47] Significantly, the spirolactam **55** was found to be a potent inhibitor of influenza virus replication with an effective concentration as low as 10^{-6}–10^{-7} M against H3N2 (Hong Kong/1/68) strain. However, it required 100 times higher concentration to be effective against the H1N1 (Puerto Rico/8/32) strain. This compares well with the inhibitory activity of the hybrid inhibitor **52** against these two strains (effective concentration was as low as 8×10^{-8} and 2×10^{-6} M, respectively). The diastereomeric spirolactam **56** was found to be less active than **55**. X-ray crystallographic analysis of N8 in complex with **55** and **56** provided better understanding of the molecular basis behind the observed differences in the inhibitory activities.[47] The overall binding mode of both compounds and interactions within the active site were very similar, except for the difference in the orientation of the spirolactam ring. In the case of the N8: **55** complex, the interactions between the spirolactam ring and the enzyme appeared to be influenced by the zwitterionic resonance state (**55a**) adopted by the thiazolidinone ring. Stabilizing interactions between the iminium nitrogen and the acidic patch (E119, E227, E277) and a water-mediated hydrogen bond favouring the negative charge build up at the amide nitrogen create a favorable placement for the thiazolidinone ring within the active site and thus contribute to the potency of this compound (Figure 7a). However, in the case of spirolactam **56**, the orientation of the thiazolidinone ring is less favorable because it forces the carbonyl group

into the acidic patch (E119, E227, E277), leading to electrostatic repulsion and thus affecting the inhibitor binding to the enzyme active site (Figure 7b).[47]

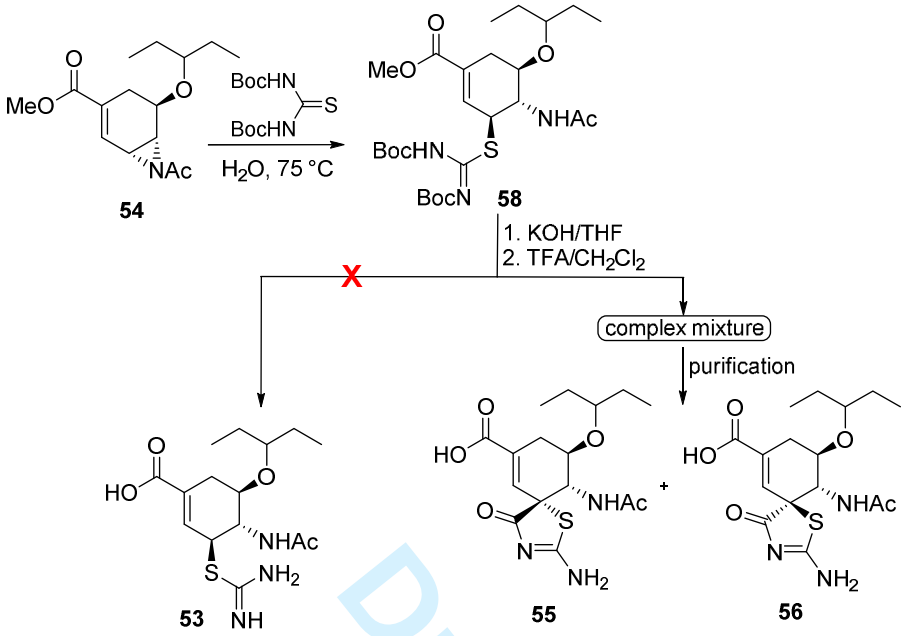

Scheme 6. Attempted synthesis of the isothiourea derivative **53**.[47]

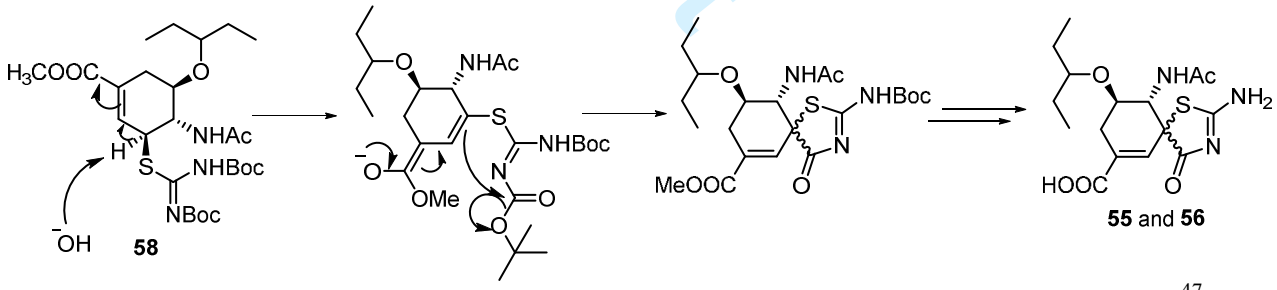

Scheme 7. Mechanism of base-catalyzed formation of diastereomeric spirolactams from **58**.[47]

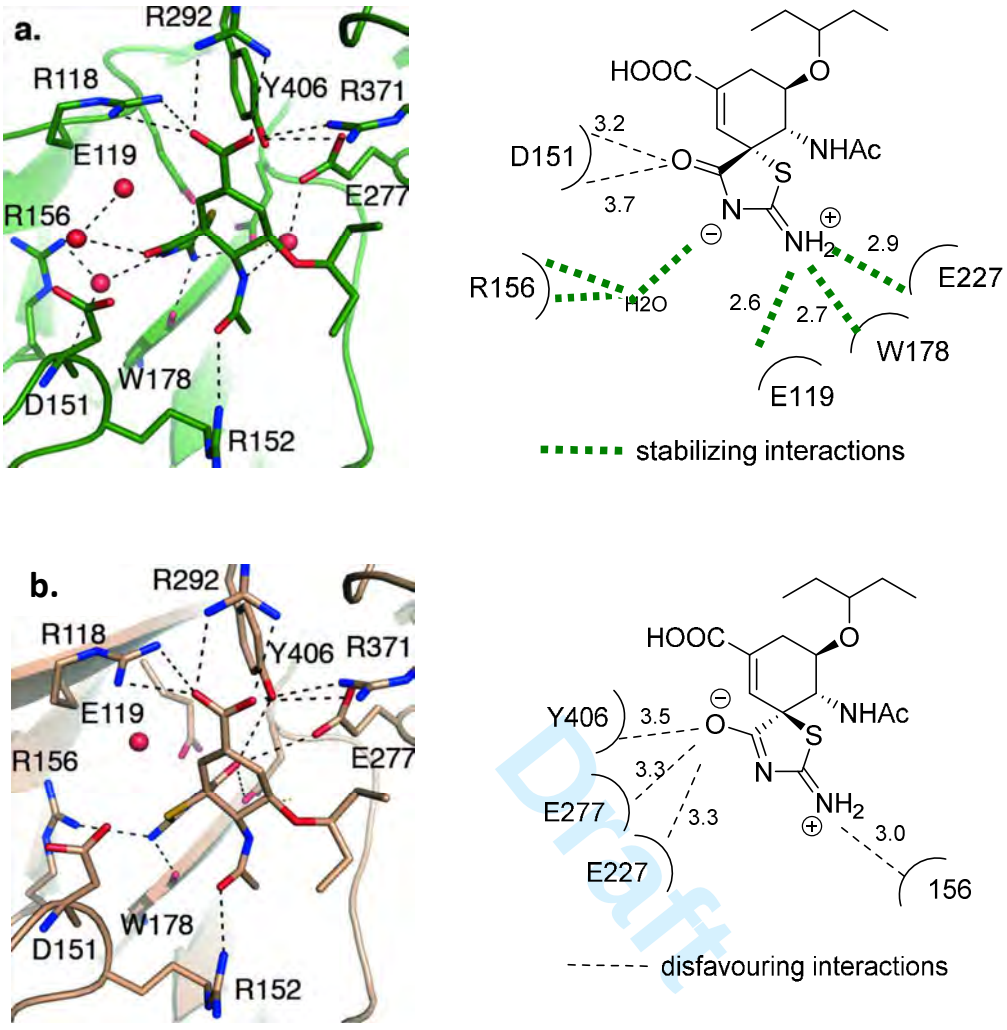

Figure 7. X-ray crystallographic analysis of a) N8:**55** and b) N8:**56** complexes.[47] Reprinted with permission from Mohan, S.; Kerry, P. S.; Bance, N.; Niikura, M.; Pinto, B. M. *Angew. Chem. Int. Ed.* **2014,** *53*, 1076-1080. Copyright © 2014, WILEY-VCH Verlag GmbH & Co. KGaA, Weinheim.

In both N8:**55** and N8:**56** complexes, the 150-loop remained in an open conformation due to steric hindrance caused by the spirolactam ring. This influence on forcing the 150-loop dynamics towards an open conformation makes the spirolactam scaffold a useful template for targeting both the catalytic site and 150 cavity.

As a final point of interest, we comment on an unusual class of bicyclic compounds designed to be neuraminidase inhibitors (**59-61**, Chart 7).[48] The parent compound **59** was designed to mimic the distorted boat conformation of the proposed transition state for the neuraminidase catalyzed reaction. Compounds **60** and **61** were designed to target both the catalytic site and 150 cavity. In the neuraminidase inhibition assay, the parent compound **59** had shown IC_{50} values of 40 and 60 μM against N2 and N1 subtypes, respectively. In comparison, compounds with 150 cavity appendages, **60** and **61**, were more active than the parent compound **59**. The IC_{50} values for **60** and **61** were determined to be 23 and 11 μM against the N2 subtype and 49 and 10 μM against the N1 subtype, respectively. However, all of them showed significantly less inhibitory activities compared to the positive control (**52**, IC_{50} = 0.78 nM).

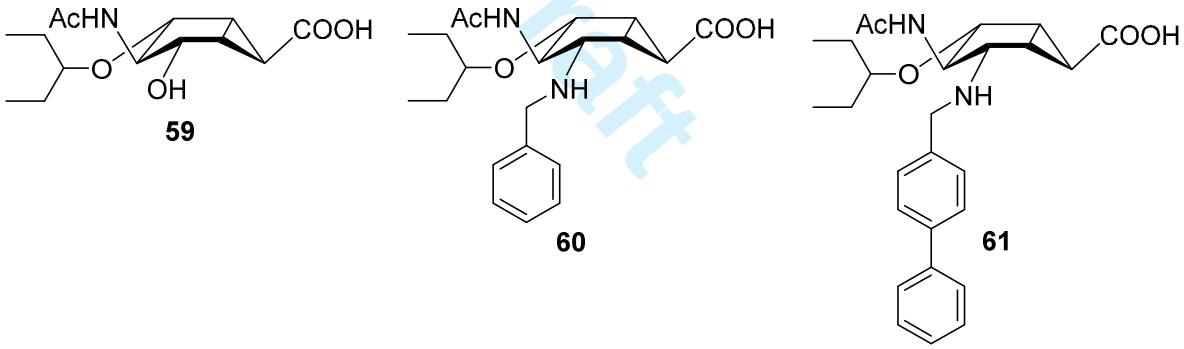

Chart 7. Neuraminidase inhibitors based on a bicyclo[3.1.0]hexane scaffold.[48]

6. Concluding remarks

Although when it was first discovered, the 150 cavity was characterized as a unique structural feature of group 1 subtypes, subsequent computational, crystallographic studies showed that it is not the case; even in group 2 enzymes one can access the 150 cavity. For example, some of the inhibitors having extended 150 cavity filling groups showed equal potency against both group 1

and group 2 enzymes, suggesting that targeting both the 150 cavity and catalytic site may work well across all subtypes and such design could lead to an universal inhibitor. Targeting the 150 cavity led to several candidate structures having oseltamivir or zanamivir scaffolds; some of these had high potency. The catalytic site binder, the carbocyclic analogue of zanamivir, with excellent inhibitory profile against a panel of wild-type and mutant neuraminidases represents a case where only a subtle variation in the core structure, namely a change in position of the double bond, can lead to a profound effect on the inhibitory profile. The spirolactam scaffold discovered serendipitously provides a new template for the design of dual-site inhibitors and opens the door for the development of neuraminidase inhibitors with improved bioavailability.

Acknowledgements

We are grateful to all our colleagues mentioned as coauthors in the cited references and to the Natural Sciences and Engineering Research Council of Canada for financial support.

References

1. World Health Organization. A revision of the system of nomenclature for influenza viruses: a W.H.O. memorandum. *Bull. World Health Organ.* **1980**, *58*, 585-591.

2. Skehel, J. J.; Wiley, D. C. *Annu. Rev. Biochem.* **2000**, *69*, 531-569.

3. (a) Bouvier, N. M.; Palese, P. *Vaccine* **2008**, *26S*, D49-D53. (b) Colman, P. M.; Varghese, J. N.; Laver, W. G. *Nature* **1983**, *303*, 41–44. (c) Varghese, J. N.; Laver, W. G.; Colman, P. M. *Nature* **1983**, *303*, 35–40.

4. (a) Treanor, J. *N. Engl. J. Med.* **2004**, *350*, 218-220. (b) Hay, A. J.; Gregory, V.; Douglas, A. R.; Lin, Y. P. *Philos. Trans. R. Soc. Lond. B Biol. Sci.* **2001**, *356*, 1861-70.

5. Centers for Disease Control and Prevention. Past pandemics. https://www.cdc.gov/flu/pandemic-resources/basics/past-pandemics.html (accessed May 2017).

6. Fouchier, R. A. M.; Munster, V.; Wallensten, A.; Bestebroer, T. M.; Herfst, S.; Smith, D.; Rimmelzwaan, G. F.; Olsen, B.; Osterhaus, A. D. M. E. *J. Virol.* **2005**, *79*, 2814-2822.

7. World Health Organization. Cumulative number of confirmed human cases of avian influenza A/(H5N1) reported to WHO.

   http://www.who.int/influenza/human_animal_interface/H5N1_cumulative_table_archives/en/ (accessed May 2017).

8. World Health Organization. Avian influenza A (H7N9) virus. http://www.who.int/influenza/human_animal_interface/influenza_h7n9/en/ (accessed May 2017).

9. Kim, C. U.; Lew, W.; Williams, M. A.; Liu, H.; Zhang, L.; Swaminathan, S.; Bischofberger, N.; Chen, M. S.; Mendel, D. B.; Tai, C. Y.; Laver, W. G.; Stevens, R. C. *J. Am. Chem. Soc.* **1997**,*119*, 681-690.

10. (a) von Itzstein, M.; Wu, W. Y.; Kok, G. B.; Pegg, M. S.; Dyason, J. C.; Jin, B.; Phan, T. V.; Smythe, M. L.; White, H. F.; Oliver, S. W.; Colman, P. M.; Varghese, J. N.; Ryan, D. M.; Woods, J. M.; Bethell, R. C.; Hotham, V. J.; Cameron, J. M.; Penn, C. R. *Nature* **1993**, *363*, 418-423. (b) von Itzstein, M.; Wu, W.-Y.; Jin, B. *Carbohydr. Res.* **1994**, *259*, 301-305.

11. Babu, Y.; Chand, P.; Bantia, S.; Kotian, P.; Dehghani, A.; El-Kattan, Y.; Lin, T. H.; Hutchison, T. L.; Elliott, A. J.; Parker, C. D.; Ananth, S. L.; Horn, L. L.; Laver, G. W.; Montgomery, J. A. *J. Med. Chem.* **2000**, *43*, 3482-3486.

12. Food and Drug Administration. Rapivab (Peramivir) information. https://www.fda.gov/Drugs/DrugSafety/InformationbyDrugClass/ucm476095.htm (accessed May2017).

13. Jefferson, T.; Jones, M. A.; Doshi, P.; Del Mar, C. B.; Hama, R.; Thompson, M. J.; Spencer, E. A.; Onakpoya, I. J.; Mahtani, K. R.; Nunan, D.; Howick, J.; Heneghan, C. J. Cochrane Database Syst. Rev. **2014**, issue 4, Art No: CD008965.

14. Le, Q. M., et al. *Nature* **2005**, *437*, 1108-1108.

15. Maenza, J.; Flexner, C. *Am Fam Physician.* **1998**, 57, 2789-2798.

16. Thompson, J. D.; Higgins, D. G.; Gibson, T. J. *Comput. Appl. Biosci.* **1994**, *10*, 19–29.

17. Baker, A. T.; Varghese, J. N.; Laver, W. G.; Air, G. M.; Colman, P. M. *Proteins* **1987**, *2*, 111-117.

18. Burmeister, W. P.; Ruigrok, R. W.; Cusack, S. *EMBO J.* **1992**, *11*, 49-56.

19. Russell, R. J.; Haire, L. F.; Stevens, D. J.; Collins, P. J.; Lin, Y. P.; Blackburn, G. M.; Hay, A. J.; Gamblin, S. J.; Skehel, J. J. *Nature* **2006**, *443*, 45-49.

20. (a) Amaro, R. E.; Minh, D. D.; Cheng, L. S.; Lindstrom, W. M. Jr.; Olson, A. J.; Lin, J. H.; Li, W. W.; McCammon, J. A. *J. Am. Chem. Soc.* **2007**, *129*, 7764-7765. (b) Amaro, R. E.; Cheng, X.; Ivanov, I.; Xu, D.; McCammon, J. A. *J. Am. Chem. Soc.* **2009**, *131*, 4702-4709.

21. (a) Amaro, R. E. et al., *Nat. Commun.* **2011**, *2*, 388. (b) Wu, Y.; Qin, G.; Gao, F.; Liu, Y.; Vavricka, C. J.; Qi, J.; Jiang, H.; Yu, K.; Gao, G. F. *Sci. Rep.* **2013**, *3*, 1551.

22. Mohan, S.; McAtamney, S.; Haselhorst, T.; Von Itzstein, M.; Pinto, B. M. *J. Med. Chem.* **2010**, *53*, 7377-7391.

23. (a) Landon, M. R.; Amaro, R. E.; Baron, R.; Ngan, C. H.; Ozonoff, D.; McCammon, J. A.; Vajda, S. *Chem. Biol. Drug Des.* **2008**, *71*, 106-116. (b) Cheng, L. S.; Amaro, R. E.; Xu, D.; Li, W. W.; Arzberger, P. W.; McCammon, J. A. *J. Med. Chem.* **2008**, *51*, 3878-3894.

24. Lew, W.; Chen, X. W.; Kim, C. U. *Curr. Med. Chem.* **2000**, *7*, 663-672.

25. Hata, K.; Koseki, K.; Yamaguchi, K.; Moriya, S.; Suzuki, Y.; Yingsakmongkon, S.; Hirai, G.; Sodeoka, M.; Von Itzstein, M.; Miyagi, T. *Antimicrob. Agents Chemother.* **2008**, *52*, 3484-3491.

26. Albohy, A.; Mohan, S.; Zheng, R. B.; Pinto, B. M.; Cairo, C. W. *Bioorg. Med. Chem.* **2011**, *19*, 2817–2822.

27. Niikura, M.; Bance, N.; Mohan, S.; Pinto, B. M. *Antiviral Res.* **2011**, *90*, 160−163.

28. Kerry, P. S.; Mohan, S.; Russell, R. J. M.; Bance, N.; Niikura, M.; Pinto, B. M. *Sci. Rep.* **2013**, *3*, 2871.

29. Greenway, K. T.; LeGresley, E. B.; Pinto, B. M. *PloS ONE* **2013**, *8*, e59873.

30. Adabala, P. J. P.; LeGresley, E. B.; Bance, N.; Niikura, M.; Pinto, B. M. *J. Org. Chem.* **2013**, *78*, 10867-10877.

31. Mooney, C. A.; Johnson, S. A.; Hart, P.; van Ufford, L. Q.; de Haan, C. A. M.; Moret, E. E.; Martin, N. I. *J. Med. Chem.* **2014**, *57*, 3154−3160.

32. Xie, Y.; Xu, D.; Huang, B.; Ma, X.; Qi, W.; Shi, F.; Liu, X.; Zhang, Y.; Xu, W. *J. Med. Chem.* **2014**, *57*, 3154−3160.

33. Wen, W.-H.; Wang, S.-Y.; Tsai, K.-C.; Cheng, Y.-S. E.; Yang, A.-S.; Fang, J.-M.; Wong, C.-H. *Bioorg. Med. Chem.* **2010**, *18*, 4074-4084.

34. Rudrawar, S.; Dyason, J. C.; Rameix-Welti, M.-A.; Rose, F. J.; Kerry, P. S.; Russell, R. J. M.; van der Werf, S.; Thomson, R. J.; Naffakh, N.; von Itzstein, M. *Nat. Commun.* **2010**, *1*, 113.

35. Rudrawar, S.; Kerry, P. S.; Rameix-Welti, M.-A.; Maggioni, A.; Dyason, J. C.; Rose, F. J.; van der Werf, S.; Thomson, R. J.; Naffakh, N.; Russell, R. J. M.; von Itzstein, M. *Org. Biomol. Chem.* **2012**, *10*, 8628-8639.

36. Rudrawar, S.; Dyason, J. C.; Maggioni, A.; Thomson, R. J.; M.; von Itzstein, M. Bioorg. *Med. Chem.* **2013**, *21*, 4820–4830.

37. Wu, Y.; Vavricka, C. J.; Wu, Y.; Li, Q.; Rudrawar, S.; Thomson, R. J.; von Itzstein, M.; Gao, G. F.; Qi, J. *Protein Cell* **2015**, *6*, 771–773.

38. Lin, C. H.; Chang, T. C.; Das, A.; Fang, M. Y.; Hung, H. C.; Hsu, K. C.; Yang, J. M.; von Itzstein, M.; Mong, K. K. T.; Hsu, T. A.; Lin, C. C. *Org. Biomol. Chem.* **2013**, *11*, 3943-3948.

39. Das, A.; Adak, A. K.; Ponnapalli, K.; Lin, C. H.; Hsu, K. C.; Yang, J. M.; Hsu, T. A.; Lin, C. C. *Eur. J. Med. Chem.* **2016**, *123*, 397-406.

40. Collins, P. J.; Haire, L.F.; Lin, Y. P.; Liu, J.; Russell, R. J.; Walker, P. A.; Skehel, J. J.; Martin, S. R.; Hay, A. J.; Gamblin, S. J. *Nature* **2008**, *453*, 1258-1262.

41. Gubareva, L. V.; Webster, R. G.; Hayden, F. G. *Antimicrob. Agents Chemother.* **2001**, *45*, 3403–3408.

42. Shie, J. J. *et al. J. Am. Chem. Soc.* **2007**, *129*, 11892–11893.

43. Wu, Y.; Gao, F.; Qi, J.; Bi, Y.; Fu, L.; Mohan, S.; Chen, Y.; Li, X.; Pinto, B. M.; Vavricka, C. J.; Tien, P.; Gao, G. F. *J. Virol.* **2016**, *90*, 10693-10700.

44. Wu, Y.; Mohan, S.; Pinto, B. M.; Gao, G. F. *unpublished results.*

45. Yen, H. L.; Mohan, S.; Pinto, B. M.; Peiris, M. *unpublished results.*

46. Wu, Y. *et al*., Cell Res. **2013**, *23*, 1347-1355.

47. Mohan, S.; Kerry, P. S.; Bance, N.; Niikura, M.; Pinto, B. M. *Angew. Chem. Int. Ed.* **2014,** *53*, 1076-1080.

48. Colombo, C.; Pinto, B. M.; Bernardi, A.; Bennet, A. J. *Org. Biomol. Chem.* **2016**, *14*, 6539-6553.